

Blue Straggler Stars: Setting up a Dynamical Clock for Open Clusters

Khushboo Kunwar RAO^{1,*}, Kaushar VAIDYA¹, Manan AGARWAL², Shanmuga BALAN¹
and Souradeep BHATTACHARYA³

¹ Department of Physics, Birla Institute of Technology and Science-Pilani, 333031 Rajasthan, India

² Anton Pannekoek Institute Universiteit van Amsterdam, Netherlands

³ Inter University Centre for Astronomy and Astrophysics, Ganeshkhind, Post Bag 4, Pune 411007, India

* Corresponding author: p20170419@pilani.bits-pilani.ac.in

This work is distributed under the Creative Commons CC-BY 4.0 Licence.

Paper presented at the 3rd BINA Workshop on “Scientific Potential of the Indo-Belgian Cooperation”, held at the Graphic Era Hill University, Bhimtal (India), 22nd–24th March 2023.

Abstract

Blue straggler stars are late bloomers that are bluer and brighter than the main sequence turnoff stars on a color-magnitude diagram of a cluster. Being a massive population compared to their other cluster siblings, their sedimentation level has been used to probe the dynamical evolution of globular clusters. In a series of studies, we explored the dynamical evolution of old open clusters, for the first time, making use of this same trait of the BSS that they settle quicker in the cluster core than any other cluster population. In these works, we have compared the theoretical estimation of dynamical ages, N_{relax} , with the observed signatures of blue straggler stars segregation either by placing open clusters in Family I/II/III classification of dynamical ages defined in globular clusters or by estimating the area enclosed between the cumulative radial distributions of BSS and another reference population in 23 open clusters.

Keywords: Blue Straggler Stars, Open Clusters, Dynamics

1. Introduction

Blue straggler stars (BSS) are core-hydrogen-burning stars that are brighter and bluer than the main sequence turnoff (MSTO) on the color-magnitude diagram (CMD) of a cluster (Sandage, 1953). This region of the CMD is forbidden according to the standard single stellar evolution theory. Therefore, their unusual location on the CMD suggests that they have a history that has increased their luminosities and temperatures. There are currently three accepted formation channels, such as stellar collisions (Hills and Day, 1976), mass transfer in a binary system whose one star is on the main sequence (MS; McCrea, 1964), and triple system evolution (Perets and Fabrycky, 2009; Naoz and Fabrycky, 2014; Portegies Zwart and Leigh, 2019).

Being the most massive objects (Shara et al., 1997), BSS residing in clustered environments are subjected to large dynamical friction and hence segregate faster in the cluster core than any other cluster population. Ferraro et al. (2012) classified globular clusters (GCs) into three distinct families of dynamical ages based on the shape of double normalized radial distributions of BSS against a reference population (REF), (i) Family I GCs – flat BSS radial distribution and hence dynamically young clusters, (ii) Family II GCs – bimodal radial distributions and hence intermediate dynamical age, and (iii) Family III – unimodal BSS radial distributions and hence dynamically old clusters. The idea behind this is to compare the frequency of BSS against another massive REF at varying radial distances from the center of the cluster to gauge the effect of dynamical friction on the BSS as opposed to that on the REF. This task demands us to bin the data of BSS and REF, which becomes particularly challenging in most open clusters (OCs) due to their smaller number of BSS.

Alessandrini et al. (2016) proposed a new parameter, A^+ , based on N -body simulations of GCs with different fractions of dark remnants (neutron stars and black holes) to measure the sedimentation level of the BSS. A^+ is the area confined between the cumulative radial distributions of the BSS and a REF, given as

$$A^+ = \int_{x_{\min}}^{x_{\max}} \phi_{\text{BSS}}(x') - \phi_{\text{REF}}(x') dx'$$

where x_{\max} and x_{\min} are the outermost and innermost radii from the cluster center, respectively. Alessandrini et al. (2016) also demonstrated that A^+ always increases with time. Stellar populations of a cluster differentially experience the strength of the Galactic field, therefore, the inner region of a cluster is least responsive to the Galactic field and hence most susceptible to mass segregation due to two-body relaxation. Therefore, we estimated A^+ up to the half-mass radius, r_h , for OCs, as was done for GCs (Lanzoni et al., 2016), and hence called it A_{rh}^+ .

BSS have been used to estimate dynamical ages of $\sim 33\%$ population of GCs of the Galaxy (Lanzoni et al., 2016; Ferraro et al., 2018, 2020; Singh and Yadav, 2019; Singh et al., 2021), however, OCs are still unexplored systems in this domain, therefore, we have undertaken this study on OCs. In this article, we summarize our work of investigating the dynamical ages of OCs from a series of three works Vaidya et al. (2020, hereafter Paper I), Rao et al. (2021, hereafter Paper II), and Rao et al. (in submission, hereafter Paper III).

2. Data Used and Membership Identification

This work has been done in three consecutive stages with the available *Gaia* data to identify members of OCs. For seven target OCs of Paper I, we identified members using the deterministic approach on *Gaia* DR2 data (Gaia Collaboration et al., 2018) that is based on the proper motions and parallaxes of *Gaia* data. For 11 target OCs of Paper II, we used cluster members and BSS of eight OCs from the literature (Paper I; Bhattacharya et al., 2019) and identified members of four OCs using the deterministic approach on *Gaia* DR2 data developed in Paper I while their BSS are taken from literature (Geller et al., 2015; Rain et al., 2020, 2021; Nine et al., 2020). To identify members of 23 target OCs of Paper III, we used the machine-learning based

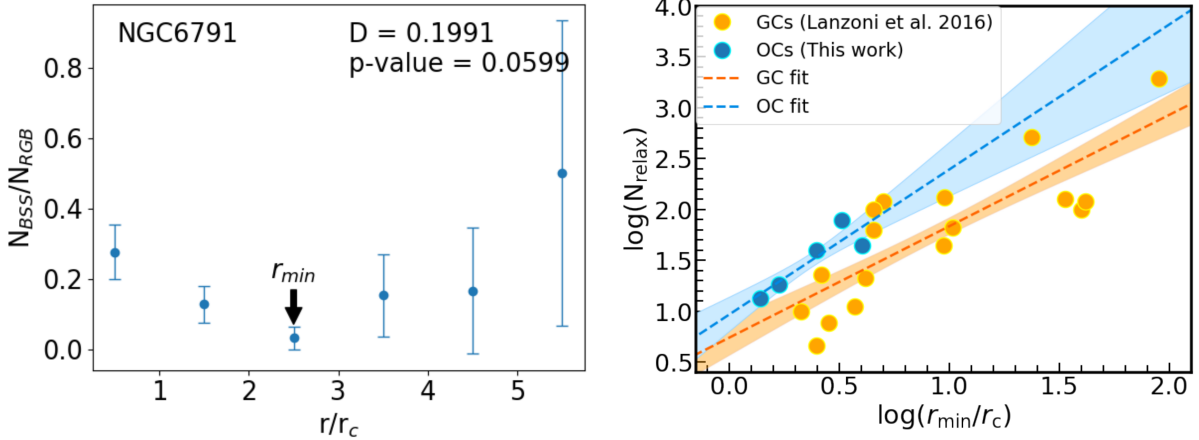


Figure 1: (Left) The ratio $N_{\text{BSS}}/N_{\text{RGB}}$ plotted against the radial distance in the units of core radius, r_c , for the NGC 6791 OC (Paper I). The error bars represent Poisson errors. The dip statistic, D , and the p -value from the dip test for bimodality are mentioned on the plots. Reproduced from Fig. 8 of Paper I (Vaidya et al., 2020). (Right) The correlation between r_{\min}/r_c and N_{relax} for five OCs (in blue) and 21 GCs (in orange) of Ferraro et al. (2012). Adapted from Fig. 9 of Paper I (Vaidya et al., 2020).

membership determination algorithm for open clusters, called ML-MOC (Agarwal et al., 2021), on *Gaia* EDR3 data (Gaia Collaboration et al., 2021).

3. Results and Discussions

3.1. Determination of dynamical ages of seven OCs using BSS radial distribution

For this analysis (Paper I), we used seven OCs that have $\text{BSS} \geq 15$. We selected BSS as the sources which are brighter and bluer than the MSTO point and red giant branch stars (RGBs) as the sources brighter than the end of the sub giant branch (SGB). Details of this method can be found in Paper I. We then plotted normalized BSS radial distribution ($N_{\text{BSS}}/N_{\text{RGB}}$) as shown in the left panel of Fig. 1 for a representative OC NGC 6791.

In order to avoid the effect of incompleteness in radial distributions, we used BSS and RGBs within the same magnitude range. The normalized BSS radial distribution shows a central peak that is decreasing until a certain radius, r_{\min} , and rises again beyond this radius. Of the seven OCs, five are found to have a bimodal radial distribution like the left panel of Fig. 1, with minima located at different distances from the center, and the remaining two OCs show flat BSS radial distributions. The Hartigan dip statistic test (Hartigan and Hartigan, 1985) performed to assess the bimodality confirms it in five OCs but fails in two OCs.

We plotted the values of r_{\min} against N_{relax} for the five OCs having bimodal BSS radial distributions as shown in the right panel of Fig. 1, where N_{relax} is defined as the number of current central relaxations occurred since cluster formation (C_{Age}/t_{rc}). The best-fit relation for

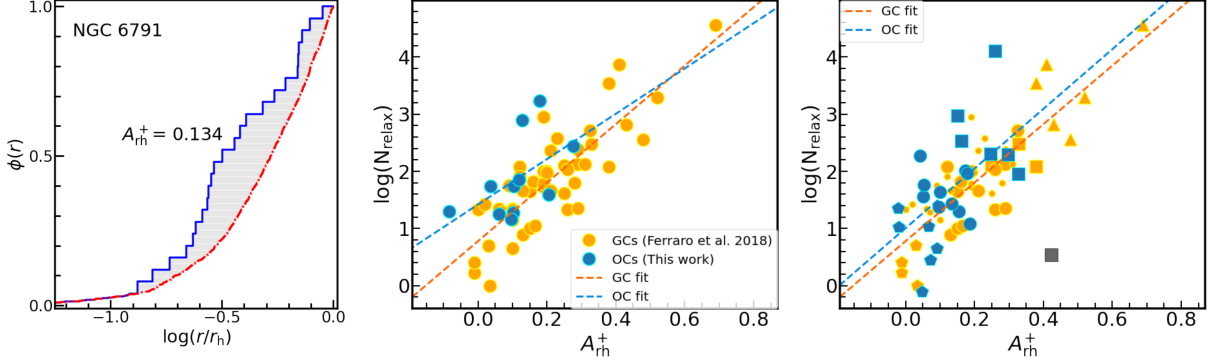


Figure 2: (Left) Cumulative radial distributions of the BSS (blue curve) and the reference population (red dashed-dotted curve) – plotted against the logarithm of the radial distance from the cluster center in the units of r_h – for NGC 6791 OC. The value of A_{rh}^+ shown on the plot corresponds to the grey-shaded portion. (Middle) A comparison of correlations between the values of A_{rh}^+ and N_{relax} for 11 OCs (Paper II) (blue color) and for 48 GCs (orange color). The blue dashed and orange dashed lines represent the best-fitted correlations for OCs and GCs, respectively. This figure is reproduced from Fig. 4 of Paper II (Rao et al., 2021, originally published in MNRAS, ©The authors, used with permission). (Right) Same as the middle panel with a bigger sample size (Paper III). The grey filled square shows Melotte 66 OC which is excluded from the fit. A detailed explanation of different markers is given in Section 3.3.

OCs data points, shown as a blue dashed line, is given as:

$$\log(N_{\text{relax}}) = 1.31(\pm 0.35) \log(r_{\min}/r_c) + 1.05(\pm 0.15) \quad (1)$$

whereas the best-fit relation for GCs data points, shown as a orange dashed line, is given as:

$$\log(N_{\text{relax}}) = 1.09(\pm 0.16) \log(r_{\min}/r_c) + 0.7(\pm 0.17). \quad (2)$$

From Eqs. (1) and (2), we see that OCs exhibit a higher intercept compared to GCs, whereas the slope is the same within the errors. With this investigation, we demonstrated that BSS radial distribution can also be used as a dynamical clock for OCs.

3.2. Determination of dynamical ages of 11 OCs using the A^+ parameter

In this work (Paper II), we used an alternative approach of using the A_{rh}^+ parameter to estimate the sedimentation level of BSS of 11 OCs having $\text{BSS} \geq 10$. To estimate A_{rh}^+ , we use MSTO, SGBs, RGBs, and red clump stars (RCs) as REF. For a detailed description of selecting BSS and REF, readers are referred to Paper II. Figure 2 (left panel) shows cumulative radial distributions of BSS and REF for a representative cluster, NGC 6791 OC. To investigate how A_{rh}^+ correlate with N_{relax} , we show the plot of A_{rh}^+ against N_{relax} in the middle panel of Fig. 2 for

these 11 OCs (blue filled circle). In order to compare OCs correlation, we have also shown GCs data points (orange filled circles). The best-fit relation for 11 OCs is given as

$$\log(N_{\text{relax}}) = 4.0(\pm 2.1) \times A_{\text{rh}}^+ + 1.42(\pm 0.30) \quad (3)$$

whereas the best-fit relation for 48 GCs is given as

$$\log(N_{\text{relax}}) = 5.1(\pm 0.5) \times A_{\text{rh}}^+ + 0.79(\pm 0.12). \quad (4)$$

OCs are found to exhibit a broad positive correlation and fall among the less evolved GCs. OCs and GCs are two vastly different systems in terms of age (OCs – 10^5 – 10^9 years, GCs – 12–13 Gyr), stellar density, member stars (OCs – up to a few thousand, GCs – up to a few hundred thousands). Because of the high density, GCs have enough gravitational force to resist the tidal force and remain in a spherical shape (Freeman and Norris, 1981) while sparser OCs are more easily stretched by the external forces and spread out over time (Chen et al., 2004). We calculate Pearson and Spearman rank correlations to compare OCs with less evolved GCs using the COCOR tool (see Paper II) as the direct comparison is insignificant due to a big difference in the sample sizes. From this, we find that the sample size of OCs needs to be increased to strengthen this correlation for OCs.

3.3. Determination of dynamical ages of 23 OCs using the A^+ parameter

In Paper III, we increase the sample size to 23 OCs, twice the sample size used in Paper II. In this work, we used MS stars of $G \geq 18.5$ mag, MSTOs, SGBs, RGBs, and RCs as REF. We then plotted values A_{rh}^+ against N_{relax} in the right panel of Fig. 2 for 23 OCs (blue) considered in this analysis. The structural and dynamical parameters for these 23 OCs are estimated following Paper II. We also showed GCs data points (orange) on this plot. We exclude Melotte 66 (grey) from the fit fit. It has the highest A_{rh}^+ , but too small N_{relax} . We speculate about possible reasons for such an anomaly in our Paper III. The best-fit relation for the remaining 22 OCs is given as

$$\log(N_{\text{relax}}) = 5.2(\pm 1.8) \times A_{\text{rh}}^+ + 1.01(\pm 0.28). \quad (5)$$

From Eqs. (4) and (5), we observe that the slope of the best-fit relation between A_{rh}^+ and N_{relax} for OCs is similar to GCs, however, errors in the slope and intercept values are still large. Compared to Eq. (3), we have marginally smaller errors, as well as slope and intercept values are closer to those found in the GCs correlation.

We can classify OCs into three different classes of dynamical ages by comparing their A_{rh}^+ and N_{relax} values to those of previously classified GCs into different dynamical ages by Ferraro et al. (2012) and Ferraro et al. (2018): (i) Class I – least evolved OCs (filled pentagons) – that populate the same space in the A_{rh}^+ vs. N_{relax} diagram as the Family I GCs (dynamically young), (ii) Class II – intermediate dynamical age I OCs (filled circles) – are intermixed with the Family II GCs (intermediate dynamical age), and (iii) Class III – intermediate dynamical age II OCs (filled squares) – that are in advanced stages of their evolution and intermixed with the Family III GCs (evolved). The Family II GCs (M92 and NGC 6752) that coincide with Family III GCs are in advanced stages of intermediate-age dynamical evolution, with the majority of the BSS segregated in the cluster center (Ferraro et al., 2012).

4. Summary

We have demonstrated that the sedimentation level of BSS can be used to determine dynamical ages of OCs (having $BSS \geq 10$).

1. The locations of minima in bimodal BSS distributions, r_{\min} , correlate well with N_{relax} in OCs too.
2. The correlation between the observed segregation of BSS with respect to reference population up to the half-mass radius, A_{rh}^+ , and N_{relax} for OCs is consistent with the known correlation between the same quantities for GCs, but with larger errors.
3. Using the estimated A_{rh}^+ and N_{relax} values, the OCs are classified into three classes of dynamical evolution.

Acknowledgments

We thank the anonymous referee for their valuable comments. SB is funded by the INSPIRE Faculty Award (DST/INSPIRE/04/2020/002224), Department of Science and Technology (DST), Government of India. This work has made use of the early third data release from the European Space Agency (ESA) mission *Gaia* (<https://www.cosmos.esa.int/gaia>), Gaia EDR3 (Gaia Collaboration et al., 2021), processed by the *Gaia* Data Processing and Analysis Consortium (DPAC, <https://www.cosmos.esa.int/web/gaia/dpac/consortium>). This research has made use of the VizieR catalog access tool, CDS, Strasbourg, France. This research also made use of the Astrophysics Data System (ADS) governed by NASA (<https://ui.adsabs.harvard.edu>).

Further Information

Authors' ORCID identifiers

0000-0001-7470-9192 (Khushboo Kunwar RAO)
0000-0003-4662-5463 (Kaushar VAIDYA)
0000-0001-6965-8642 (Manan AGARWAL)
0000-0003-4594-6943 (Souradeep BHATTACHARYA)

Author contributions

Khushboo K. Rao – Conceptualization, Data curation, Formal Analysis, Investigation, Methodology, Software, Validation, Visualization, Writing; original draft, Writing; review and editing
Kaushar Vaidya – Conceptualization, Data curation, Formal Analysis, Supervision, Validation, Visualization, Writing; original draft, Writing; review and editing

Manan Agarwal – Data curation, Software, Visualization, Writing; review and editing

Shanmuga Balan – Data curation, Writing; review and editing

Souradeep Bhattacharya – Validation, Visualization, Writing; review and editing

Conflicts of interest

The authors declare no conflict of interest.

References

- Agarwal, M., Rao, K. K., Vaidya, K. and Bhattacharya, S. (2021) ML-MOC: Machine learning (kNN and GMM) based membership determination for open clusters. *MNRAS*, 502(2), 2582–2599. <https://doi.org/10.1093/mnras/stab118>.
- Alessandrini, E., Lanzoni, B., Ferraro, F. R., Miocchi, P. and Vesperini, E. (2016) Investigating the mass segregation process in globular clusters with blue straggler stars: The impact of dark remnants. *ApJ*, 833(2), 252. <https://doi.org/10.3847/1538-4357/833/2/252>.
- Bhattacharya, S., Vaidya, K., Chen, W. P. and Beccari, G. (2019) The blue straggler population of the old open cluster Berkeley 17. *A&A*, 624, A26. <https://doi.org/10.1051/0004-6361/201834449>.
- Chen, W. P., Chen, C. W. and Shu, C. G. (2004) Morphology of Galactic open clusters. *AJ*, 128(5), 2306–2315. <https://doi.org/10.1086/424855>.
- Ferraro, F. R., Lanzoni, B. and Dalessandro, E. (2020) The “dynamical clock”: dating the internal dynamical evolution of star clusters with blue straggler stars. *arXiv e-prints*, arXiv:2001.07435.
- Ferraro, F. R., Lanzoni, B., Dalessandro, E., Beccari, G., Pasquato, M., Miocchi, P., Rood, R. T., Sigurdsson, S., Sills, A., Vesperini, E., Mapelli, M., Contreras, R., Sanna, N. and Mucciarelli, A. (2012) Dynamical age differences among coeval star clusters as revealed by blue stragglers. *Natur*, 492(7429), 393–395. <https://doi.org/10.1038/nature11686>.
- Ferraro, F. R., Lanzoni, B., Raso, S., Nardiello, D., Dalessandro, E., Vesperini, E., Piotto, G., Pallanca, C., Beccari, G., Bellini, A., Libralato, M., Anderson, J., Aparicio, A., Bedin, L. R., Cassisi, S., Milone, A. P., Ortolani, S., Renzini, A., Salaris, M. and van der Marel, R. P. (2018) The Hubble Space Telescope UV legacy survey of galactic globular clusters. XV. The dynamical clock: Reading cluster dynamical evolution from the segregation level of blue straggler stars. *ApJ*, 860(1), 36. <https://doi.org/10.3847/1538-4357/aac01c>.
- Freeman, K. C. and Norris, J. (1981) The chemical composition, structure, and dynamics of globular clusters. *ARA&A*, 19, 319–356. <https://doi.org/10.1146/annurev.aa.19.090181.001535>.
- Gaia Collaboration, Brown, A. G. A., Vallenari, A., Prusti, T., de Bruijne, J. H. J., Babusiaux, C., Bailer-Jones, C. A. L., Biermann, M., Evans, D. W., Eyer, L., Jansen, F., Jordi, C., Klioner, S. A., Lammers, U., Lindegren, L., Luri, X., Mignard, F., Panem, C., Pourbaix, D., Randich, S., Sartoretti, P., Siddiqui, H. I., Soubiran, C., van Leeuwen, F., Walton, N. A., Arenou, F., Bastian, U., Cropper, M., Drimmel, R., Katz, D., Lattanzi, M. G., Bakker, J.,

Cacciari, C., Castañeda, J., Chaoul, L., Cheek, N., De Angeli, F., Fabricius, C., Guerra, R., Holl, B., Masana, E., Messineo, R., Mowlavi, N., Nienartowicz, K., Panuzzo, P., Portell, J., Riello, M., Seabroke, G. M., Tanga, P., Thévenin, F., Gracia-Abril, G., Comoretto, G., Garcia-Reinaldos, M., Teyssier, D., Altmann, M., Andrae, R., Audard, M., Bellas-Velidis, I., Benson, K., Berthier, J., Blomme, R., Burgess, P., Busso, G., Carry, B., Cellino, A., CLEMENTINI, G., Clotet, M., Creevey, O., Davidson, M., De Ridder, J., Delchambre, L., Dell’Oro, A., Ducourant, C., Fernández-Hernández, J., Fouesneau, M., Frémat, Y., Galluccio, L., García-Torres, M., González-Núñez, J., González-Vidal, J. J., Gosset, E., Guy, L. P., Halbwachs, J. L., Hambly, N. C., Harrison, D. L., Hernández, J., Hestroffer, D., Hodgkin, S. T., Hutton, A., Jasniewicz, G., Jean-Antoine-Piccolo, A., Jordan, S., Korn, A. J., Krone-Martins, A., Lanzafame, A. C., Lebzelter, T., Löffler, W., Manteiga, M., Marrese, P. M., Martín-Fleitas, J. M., Moitinho, A., Mora, A., Muinonen, K., Osinde, J., Pancino, E., Pauwels, T., Petit, J. M., Recio-Blanco, A., Richards, P. J., Rimoldini, L., Robin, A. C., Sarro, L. M., Siopis, C., Smith, M., Sozzetti, A., Süveges, M., Torra, J., van Reeven, W., Abbas, U., Abreu Aramburu, A., Accart, S., Aerts, C., Altavilla, G., Álvarez, M. A., Alvarez, R., Alves, J., Anderson, R. I., Andrei, A. H., Anglada Varela, E., Antiche, E., Antoja, T., Arcay, B., Astraatmadja, T. L., Bach, N., Baker, S. G., Balaguer-Núñez, L., Balm, P., Barache, C., Barata, C., Barbato, D., Barblan, F., Barklem, P. S., Barrado, D., Barros, M., Barstow, M. A., Bartholomé Muñoz, S., Bassilana, J. L., Becciani, U., Bellazzini, M., Berihuete, A., Bertone, S., Bianchi, L., Bienaymé, O., Blanco-Cuaresma, S., Boch, T., Boeche, C., Bombrun, A., Borrachero, R., Bossini, D., Bouquillon, S., Bourda, G., Bragaglia, A., Bramante, L., Breddels, M. A., Bressan, A., Brouillet, N., Brüsemeister, T., Brugaletta, E., Bucciarelli, B., Burlacu, A., Busonero, D., Butkevich, A. G., Buzzi, R., Caffau, E., Cancelliere, R., Cannizzaro, G., Cantat-Gaudin, T., Carballo, R., Carlucci, T., Carrasco, J. M., Casamiquela, L., Castellani, M., Castro-Ginard, A., Charlot, P., Chemin, L., Chiavassa, A., Cocozza, G., Costigan, G., Cowell, S., Crifo, F., Crosta, M., Crowley, C., Cuypers, J., Dafonte, C., Damerdji, Y., Dapergolas, A., David, P., David, M., de Laverny, P., De Luise, F., De March, R., de Martino, D., de Souza, R., de Torres, A., Debosscher, J., del Pozo, E., Delbo, M., Delgado, A., Delgado, H. E., Di Matteo, P., Diakite, S., Diener, C., Distefano, E., Dolding, C., Drazinos, P., Durán, J., Edvardsson, B., Enke, H., Eriksson, K., Esquej, P., Eynard Bontemps, G., Fabre, C., Fabrizio, M., Faigler, S., Falcão, A. J., Farràs Casas, M., Federici, L., Fedorets, G., Fernique, P., Figueras, F., Filippi, F., Findeisen, K., Fonti, A., Fraile, E., Fraser, M., Frézouls, B., Gai, M., Galleti, S., Garabato, D., García-Sedano, F., Garofalo, A., Garralda, N., Gavel, A., Gavras, P., Gerssen, J., Geyer, R., Giacobbe, P., Gilmore, G., Girona, S., Giuffrida, G., Glass, F., Gomes, M., Granvik, M., Gueguen, A., Guerrier, A., Guiraud, J., Gutiérrez-Sánchez, R., Haigron, R., Hatzidimitriou, D., Hauser, M., Haywood, M., Heiter, U., Helmi, A., Heu, J., Hilger, T., Hobbs, D., Hofmann, W., Holland, G., Huckle, H. E., Hypki, A., Icardi, V., Janßen, K., Jevardat de Fombelle, G., Jonker, P. G., Juhász, Á. L., Julbe, F., Karampelas, A., Kewley, A., Klar, J., Kochoska, A., Kohley, R., Kolenberg, K., Kontizas, M., Kontizas, E., Koposov, S. E., Kordopatis, G., Kostrzewska-Rutkowska, Z., Koubek, P., Lambert, S., Lanza, A. F., Lasne, Y., Lavigne, J. B., Le Fustec, Y., Le Poncin-Lafitte, C., Lebreton, Y., Leccia, S., Leclerc, N., Lecoeur-Taibi, I., Lenhardt, H., Leroux, F., Liao, S., Licata, E., Lindstrøm, H. E. P., Lister,

T. A., Livanou, E., Lobel, A., López, M., Managau, S., Mann, R. G., Mantelet, G., Marchal, O., Marchant, J. M., Marconi, M., Marinoni, S., Marschalkó, G., Marshall, D. J., Martino, M., Marton, G., Mary, N., Massari, D., Matijevič, G., Mazeh, T., McMillan, P. J., Messina, S., Michalik, D., Millar, N. R., Molina, D., Molinaro, R., Molnár, L., Montegriffo, P., Mor, R., Morbidelli, R., Morel, T., Morris, D., Mulone, A. F., Muraveva, T., Musella, I., Nelemans, G., Nicastro, L., Noval, L., O'Mullane, W., Ordénovic, C., Ordóñez-Blanco, D., Osborne, P., Pagani, C., Pagano, I., Pailler, F., Palacin, H., Palaversa, L., Panahi, A., Pawlak, M., Piersimoni, A. M., Pineau, F. X., Plachy, E., Plum, G., Poggio, E., Poujoulet, E., Prša, A., Pulone, L., Racero, E., Ragaini, S., Rambaux, N., Ramos-Lerate, M., Regibo, S., Reylé, C., Riclet, F., Ripepi, V., Riva, A., Rivard, A., Rixon, G., Roegiers, T., Roelens, M., Romero-Gómez, M., Rowell, N., Royer, F., Ruiz-Dern, L., Sadowski, G., Sagristà Sellés, T., Sahlmann, J., Salgado, J., Salguero, E., Sanna, N., Santana-Ros, T., Sarasso, M., Savietto, H., Schultheis, M., Sciacca, E., Segol, M., Segovia, J. C., Ségransan, D., Shih, I. C., Siltala, L., Silva, A. F., Smart, R. L., Smith, K. W., Solano, E., Solitro, F., Sordo, R., Soria Nieto, S., Souchay, J., Spagna, A., Spoto, F., Stampa, U., Steele, I. A., Steidelmüller, H., Stephenson, C. A., Stoев, H., Suess, F. F., Surdej, J., Szabados, L., Szegedi-Elek, E., Tapiador, D., Taris, F., Tauran, G., Taylor, M. B., Teixeira, R., Terrett, D., Teyssandier, P., Thuillot, W., Titarenko, A., Torra Clotet, F., Turon, C., Ulla, A., Utrilla, E., Uzzi, S., Vaillant, M., Valentini, G., Valette, V., van Elteren, A., Van Hemelryck, E., van Leeuwen, M., Vaschetto, M., Vecchiatto, A., Veljanoski, J., Viala, Y., Vicente, D., Vogt, S., von Essen, C., Voss, H., Votruba, V., Voutsinas, S., Walmsley, G., Weiler, M., Wertz, O., Wevers, T., Wyrzykowski, Ł., Yoldas, A., Žerjal, M., Ziaeepour, H., Zorec, J., Zschocke, S., Zucker, S., Zurbach, C. and Zwitter, T. (2018) *Gaia* Data Release 2. Summary of the contents and survey properties. *A&A*, 616, A1. <https://doi.org/10.1051/0004-6361/201833051>.

Gaia Collaboration, Brown, A. G. A., Vallenari, A., Prusti, T., de Bruijne, J. H. J., Babusiaux, C., Biermann, M., Creevey, O. L., Evans, D. W., Eyer, L., Hutton, A., Jansen, F., Jordi, C., Klioner, S. A., Lammers, U., Lindegren, L., Luri, X., Mignard, F., Panem, C., Pourbaix, D., Randich, S., Sartoretti, P., Soubiran, C., Walton, N. A., Arenou, F., Bailer-Jones, C. A. L., Bastian, U., Cropper, M., Drimmel, R., Katz, D., Lattanzi, M. G., van Leeuwen, F., Bakker, J., Cacciari, C., Castañeda, J., De Angeli, F., Ducourant, C., Fabricius, C., Fouesneau, M., Frémat, Y., Guerra, R., Guerrier, A., Guiraud, J., Jean-Antoine Piccolo, A., Masana, E., Messineo, R., Mowlavi, N., Nicolas, C., Nienartowicz, K., Pailler, F., Panuzzo, P., Riclet, F., Roux, W., Seabroke, G. M., Sordo, R., Tanga, P., Thévenin, F., Gracia-Abril, G., Portell, J., Teyssier, D., Altmann, M., Andrae, R., Bellas-Velidis, I., Benson, K., Berthier, J., Blomme, R., Brugaletta, E., Burgess, P. W., Busso, G., Carry, B., Cellino, A., Cheek, N., Clementini, G., Damerdji, Y., Davidson, M., Delchambre, L., Dell'Oro, A., Fernández-Hernández, J., Galluccio, L., García-Lario, P., Garcia-Reinaldos, M., González-Núñez, J., Gosset, E., Haigron, R., Halbwachs, J. L., Hambly, N. C., Harrison, D. L., Hatzidimitriou, D., Heiter, U., Hernández, J., Hestroffer, D., Hodgkin, S. T., Holl, B., Janßen, K., Jevardat de Fombelle, G., Jordan, S., Krone-Martins, A., Lanzafame, A. C., Löffler, W., Lorca, A., Manteiga, M., Marchal, O., Marrese, P. M., Moitinho, A., Mora, A., Muinonen, K., Osborne, P., Pancino, E., Pauwels, T., Petit, J. M., Recio-Blanco, A., Richards, P. J., Riello, M., Rimoldini, L.,

Robin, A. C., Roegiers, T., Rybizki, J., Sarro, L. M., Siopis, C., Smith, M., Sozzetti, A., Ulla, A., Utrilla, E., van Leeuwen, M., van Reeven, W., Abbas, U., Abreu Aramburu, A., Accart, S., Aerts, C., Aguado, J. J., Ajaj, M., Altavilla, G., Álvarez, M. A., Alvarez Cid-Fuentes, J., Alves, J., Anderson, R. I., Anglada Varela, E., Antoja, T., Audard, M., Baines, D., Baker, S. G., Balaguer-Núñez, L., Balbinot, E., Balog, Z., Barache, C., Barbato, D., Barros, M., Barstow, M. A., Bartolomé, S., Bassilana, J. L., Bauchet, N., Baudesson-Stella, A., Becchiani, U., Bellazzini, M., Bernet, M., Bertone, S., Bianchi, L., Blanco-Cuaresma, S., Boch, T., Bombrun, A., Bossini, D., Bouquillon, S., Bragaglia, A., Bramante, L., Breedt, E., Bresnan, A., Brouillet, N., Bucciarelli, B., Burlacu, A., Busonero, D., Butkevich, A. G., Buzzi, R., Caffau, E., Cancelliere, R., Cánovas, H., Cantat-Gaudin, T., Carballo, R., Carlucci, T., Carnerero, M. I., Carrasco, J. M., Casamiquela, L., Castellani, M., Castro-Ginard, A., Castro Sampol, P., Chaoul, L., Charlot, P., Chemin, L., Chiavassa, A., Cioni, M. R. L., Comoretto, G., Cooper, W. J., Cornez, T., Cowell, S., Crifo, F., Crosta, M., Crowley, C., Dafonte, C., Dapergolas, A., David, M., David, P., de Laverny, P., De Luise, F., De March, R., De Ridder, J., de Souza, R., de Teodoro, P., de Torres, A., del Peloso, E. F., del Pozo, E., Delbo, M., Delgado, A., Delgado, H. E., Delisle, J. B., Di Matteo, P., Diakite, S., Diener, C., Distefano, E., Dolding, C., Eappachen, D., Edvardsson, B., Enke, H., Esquej, P., Fabre, C., Fabrizio, M., Faigler, S., Fedorets, G., Fernique, P., Fienga, A., Figueras, F., Fouron, C., Frakoudi, F., Fraile, E., Franke, F., Gai, M., Garabato, D., Garcia-Gutierrez, A., García-Torres, M., Garofalo, A., Gavras, P., Gerlach, E., Geyer, R., Giacobbe, P., Gilmore, G., Girona, S., Giuffrida, G., Gomel, R., Gomez, A., Gonzalez-Santamaria, I., González-Vidal, J. J., Granvik, M., Gutiérrez-Sánchez, R., Guy, L. P., Hauser, M., Haywood, M., Helmi, A., Hidalgo, S. L., Hilger, T., Hładcuk, N., Hobbs, D., Holland, G., Huckle, H. E., Jasniewicz, G., Jonker, P. G., Juaristi Campillo, J., Julbe, F., Karbevska, L., Kervella, P., Khanna, S., Kochoska, A., Kontizas, M., Kordopatis, G., Korn, A. J., Kostrzewska-Rutkowska, Z., Kruszyńska, K., Lambert, S., Lanza, A. F., Lasne, Y., Le Campion, J. F., Le Fustec, Y., Lebreton, Y., Lebzelter, T., Leccia, S., Leclerc, N., Lecoer-Taibi, I., Liao, S., Licata, E., Lindstrøm, E. P., Lister, T. A., Livanou, E., Lobel, A., Madrero Pardo, P., Managau, S., Mann, R. G., Marchant, J. M., Marconi, M., Marcos Santos, M. M. S., Marinoni, S., Marocco, F., Marshall, D. J., Martin Polo, L., Martín-Fleitas, J. M., Masip, A., Massari, D., Mastrobuono-Battisti, A., Mazeh, T., McMillan, P. J., Messina, S., Michalik, D., Millar, N. R., Mints, A., Molina, D., Molinaro, R., Molnár, L., Montegriffo, P., Mor, R., Morbidelli, R., Morel, T., Morris, D., Mulone, A. F., Munoz, D., Muraveva, T., Murphy, C. P., Musella, I., Noval, L., Ordénovic, C., Orrù, G., Osinde, J., Paganí, C., Pagano, I., Palaversa, L., Palicio, P. A., Panahi, A., Pawlak, M., Peñalosa Esteller, X., Penttilä, A., Piersimoni, A. M., Pineau, F. X., Plachy, E., Plum, G., Poggio, E., Poretti, E., Poujoulet, E., Prša, A., Pulone, L., Racero, E., Ragaini, S., Rainer, M., Raiteri, C. M., Rambaux, N., Ramos, P., Ramos-Lerate, M., Re Fiorentin, P., Regibo, S., Reylé, C., Ripepi, V., Riva, A., Rixon, G., Robichon, N., Robin, C., Roelens, M., Rohrbasser, L., Romero-Gómez, M., Rowell, N., Royer, F., Rybicki, K. A., Sadowski, G., Sagristà Sellés, A., Sahlmann, J., Salgado, J., Salguero, E., Samaras, N., Sanchez Gimenez, V., Sanna, N., Santoveña, R., Sarasso, M., Schultheis, M., Sciacca, E., Segol, M., Segovia, J. C., Ségransan, D., Semeux, D., Shahaf, S., Siddiqui, H. I., Siebert, A., Siltala, L., Slezak, E., Smart, R. L., Solano, E.,

Solitro, F., Souami, D., Souchay, J., Spagna, A., Spoto, F., Steele, I. A., Steidelmüller, H., Stephenson, C. A., Süveges, M., Szabados, L., Szegedi-Elek, E., Taris, F., Tauran, G., Taylor, M. B., Teixeira, R., Thuillot, W., Tonello, N., Torra, F., Torra, J., Turon, C., Unger, N., Vaillant, M., van Dillen, E., Vanel, O., Vecchiato, A., Viala, Y., Vicente, D., Voutsinas, S., Weiler, M., Wevers, T., Wyrzykowski, Ł., Yoldas, A., Yvard, P., Zhao, H., Zorec, J., Zucker, S., Zurbach, C. and Zwitter, T. (2021) *Gaia* Early Data Release 3. Summary of the contents and survey properties. *A&A*, 649, A1. <https://doi.org/10.1051/0004-6361/202039657>.

Geller, A. M., Latham, D. W. and Mathieu, R. D. (2015) Stellar radial velocities in the old open cluster M67 (NGC 2682). I. Memberships, binaries, and kinematics. *AJ*, 150(3), 97. <https://doi.org/10.1088/0004-6256/150/3/97>.

Hartigan, J. A. and Hartigan, P. M. (1985) The dip test of unimodality. *AnSta*, 13(1), 70–84. <http://www.jstor.org/stable/2241144>.

Hills, J. G. and Day, C. A. (1976) Stellar collisions in globular clusters. *ApL*, 17, 87.

Lanzoni, B., Ferraro, F. R., Alessandrini, E., Dalessandro, E., Vesperini, E. and Raso, S. (2016) Refining the dynamical clock for star clusters. *ApJ*, 833(2), L29. <https://doi.org/10.3847/2041-8213/833/2/L29>.

McCrea, W. H. (1964) Extended main-sequence of some stellar clusters. *MNRAS*, 128, 147. <https://doi.org/10.1093/mnras/128.2.147>.

Naoz, S. and Fabrycky, D. C. (2014) Mergers and obliquities in stellar triples. *ApJ*, 793(2), 137. <https://doi.org/10.1088/0004-637X/793/2/137>.

Nine, A. C., Milliman, K. E., Mathieu, R. D., Geller, A. M., Leiner, E. M., Platais, I. and Toftlemire, B. M. (2020) WIYN open cluster study. LXXXII. Radial-velocity measurements and spectroscopic binary orbits in the open cluster NGC 7789. *AJ*, 160(4), 169. <https://doi.org/10.3847/1538-3881/abad3b>.

Perets, H. B. and Fabrycky, D. C. (2009) On the triple origin of blue stragglers. *ApJ*, 697(2), 1048–1056. <https://doi.org/10.1088/0004-637X/697/2/1048>.

Portegies Zwart, S. and Leigh, N. W. C. (2019) A triple origin for twin blue stragglers in close binaries. *ApJ*, 876(2), L33. <https://doi.org/10.3847/2041-8213/ab1b75>.

Rain, M. J., Carraro, G., Ahumada, J. A., Villanova, S., Boffin, H. and Monaco, L. (2021) The blue straggler population of the open clusters Trumpler 5, Trumpler 20, and NGC 2477. *AJ*, 161(1), 37. <https://doi.org/10.3847/1538-3881/abc1ee>.

Rain, M. J., Carraro, G., Ahumada, J. A., Villanova, S., Boffin, H., Monaco, L. and Beccari, G. (2020) A study of the blue straggler population of the old open cluster Collinder 261. *AJ*, 159(2), 59. <https://doi.org/10.3847/1538-3881/ab5f0b>.

Rao, K. K., Vaidya, K., Agarwal, M. and Bhattacharya, S. (2021) Determination of dynamical ages of open clusters through the a^+ parameter – I. MNRAS, 508(4), 4919–4937. <https://doi.org/10.1093/mnras/stab2894>.

Sandage, A. R. (1953) The color-magnitude diagram for the globular cluster M 3. AJ, 58, 61–75. <https://doi.org/10.1086/106822>.

Shara, M. M., Saffer, R. A. and Livio, M. (1997) The first direct measurement of the mass of a blue straggler in the core of a globular cluster: BSS 19 in 47 Tucanae. ApJ, 489(1), L59–L62. <https://doi.org/10.1086/310952>.

Singh, G. and Yadav, R. K. S. (2019) The radial distribution of blue stragglers in Galactic globular cluster NGC 6656 – clues to the dynamical status. MNRAS, 482(4), 4874–4882. <https://doi.org/10.1093/mnras/sty2961>.

Singh, G., Yadav, R. K. S., Sahu, S. and Subramaniam, A. (2021) Study of dynamical status of the globular cluster NGC 1851 using ultraviolet imaging telescope. JApA, 42(2), 53. <https://doi.org/10.1007/s12036-021-09725-3>.

Vaidya, K., Rao, K. K., Agarwal, M. and Bhattacharya, S. (2020) Blue straggler populations of seven open clusters with *Gaia* DR2. MNRAS, 496(2), 2402–2421. <https://doi.org/10.1093/mnras/staa1667>.